THE FASEB JOURNAL • RESEARCH • www.fasebj.org

Human muscular mitochondrial fusion in athletes during exercise

Jesús R. Huertas,[*,†,1] Francisco Javier Ruiz-Ojeda,[‡,§,¶] Julio Plaza-Díaz,[†,‡,§] Nikolai B. Nordsborg,[‖] Jesús Martín-Albo,[†] Ascensión Rueda-Robles,[†] and Rafael A. Casuso[*,†,2]

[*]Department of Physiology, School of Pharmacy, [†]José Mataix Institute of Nutrition and Food Technology,Biomedical Research Centre, and [‡]Department of Biochemistry and Molecular Biology II, School of Pharmacy, University of Granada, Granada, Spain; [§]Instituto de Investigación Biosanitaria de Granada (IBS.GRANADA), Complejo Hospitalario Universitario de Granada, Granada, Spain; [¶]Adipocytes and Metabolism Unit, Institute for Diabetes and Obesity, Helmholtz Diabetes Center at Helmholtz Center Munich, Munich, Germany; and [‖]Department of Nutrition, Exercise, and Sports (NEXS), Section of Integrative Physiology, University of Copenhagen, Copenhagen, Denmark

ABSTRACT: The main objective of this work was to investigate whether mitochondrial fusion occurs in the skeletal muscle of well-trained athletes in response to high-intensity exercise. Well-trained swimmers (n = 9) performed a duration-matched sprint interval training (SIT) and high-intensity high-volume training (HIHVT) session on separate days. Muscle samples from triceps brachii were taken before, immediately after, and 3 h after the training sessions. Transmission electron microscopy (TEM) was applied to assess mitochondrial morphology. Moreover, expression of genes coding for regulators of mitochondrial fusion and fission were assessed by real-time quantitative PCR. In addition, mitofusin (MFN)2 and optic atrophy 1 (OPA1) were quantified by Western blot analysis. TEM analyses showed that mitochondrial morphology remained altered for 3 h after HIHVT, whereas SIT-induced changes were only evident immediately after exercise. Only SIT increased MFN1 and MFN2 mRNA expression, whereas SIT and HIHVT both increased MFN2 protein content 3 h after exercise. Notably, only HIHVT increased OPA1 protein content. Mitochondrial morphologic changes that suggest fusion occurs in well-adapted athletes during exercise. However, HIHVT appears as a more robust inducer of mitochondrial fusion events than SIT. Indeed, SIT induces a rapid and transient change in mitochondrial morphology.—Huertas, J. R., Ruiz-Ojeda, F. J., Plaza-Díaz, J., Nordsborg, N. B., Martín-Albo, J., Rueda-Robles, A., Casuso, R. A. Human muscular mitochondrial fusion in athletes during exercise. FASEB J. 33, 12087–12098 (2019). www.fasebj.org

KEY WORDS: physical activity · mitochondrial fission · skeletal muscle · mitofusin 2

Mitochondria are conserved organelles in eukaryotic organisms and form a complex interconnected reticulum capable of ATP production and proton-motive force energy distribution (1). Mitochondria are composed of 2 (inner and outer) membranes that enclose a matrix and an intermembrane space. In addition, the inner membrane forms invaginations projected into the matrix that are called cristae. It has recently become apparent that mitochondria are highly dynamic organelles that undergo marked morphologic changes in response to both energetic and physical stress (2, 3). Morphologic changes help to maintain a cell-like mitochondrial cycle, which involves *de novo* mitochondrial biogenesis, mitochondrial fusion, and the fragmentation of dysfunctional organelles (fission) for its breakdown by the autophagosome (mitophagy) (4).

Fusion of the inner mitochondrial membrane is regulated by optic atrophy (OPA)1, whereas fusion of the outer mitochondrial membrane is regulated by the transmembrane proteins mitofusin (MFN)1 and 2 (3). Both MFN1 and MFN2 are individually able to change their molecular conformation in order to constrain or permit mitochondrial fusion (5, 6).

Weeks or months of regular exercise training is known to increase mitochondrial content (7) and augment mitochondrial volume (8). In addition, a prolonged exercise training period also changes the morphology of the

ABBREVIATIONS: AR, aspect ratio; DRP, dynamin-like protein; FF, form factor; FIS1, fission, mitochondrial 1; HIHVT, high-intensity high-volume training; HR, heart rate; Hsp-70, heat shock protein 70; IMF, intermyofibrillar; MARCH5, membrane-associated ring finger (C3HC4) 5; MFF, mitochondrial fission factor; MFN, mitofusin; $Mito_{VD}$, mitochondrial volume density; OPA1, optic atrophy 1; PARK2, parkin RBR E3 ubiquitin protein ligase; PGC, peroxisome proliferator-activated receptor-γ coactivator; RPE, rate of perceived exertion; SIT, sprint interval training; SS, subsarcolemmal; TEM, transmission electron microscopy

[1] Correspondence: Institute of Nutrition and Food Technology "José Mataix," Biomedical Research Centre, University of Granada, Laboratory 116, Avenida del Conocimiento s/n, 18100 Granada, Spain. E-mail: jhuertas@ugr.es

[2] Correspondence: Institute of Nutrition and Food Technology "José Mataix," Biomedical Research Centre, University of Granada, Laboratory 116, Avenida del Conocimiento s/n, 18100 Granada, Spain. E-mail: casusopt@gmail.es

doi: 10.1096/fj.201900365RR
This article includes supplemental data. Please visit *http://www.fasebj.org* to obtain this information.

mitochondrial electron transport system located within the cristae (9). The morphologic changes in response to altered energetic demands appear to be of decisive importance for supporting the required cellular energy demand (3, 10). With acute exercise, cellular energetic drops induce fusion signaling events that may secure a link between oxygen-rich areas, such as the areas close to the sarcolemma, to areas with limited oxygen availability, such as the intermyofibrillar (IMF) space (11). Accordingly, mitochondrial elongation occurs in parallel with cellular energetic drops (12). Muscular oxygen demand is highly dependent on power output (13–15), and thus it seems plausible that the degree of exercise-induced mitochondrial fusion is dependent on exercise intensity. Because high-intensity exercise causes large perturbations of cellular energy demands (13–15) and engages all muscle fibers, it seems plausible that induced fusion may be more pronounced than with moderate-intensity exercise. In humans, Cartoni *et al.* (16) have reported that MFN1 and MFN2 mRNA expression was elevated for 24 h following strenuous continuous exercise. In addition, it has been observed that MFN2 mRNA expression increases immediately after sprint exercise performed as repeated 20- to 30-s all-out efforts (17, 18) as well as after 25- to 50-min moderate-intensity exercise at the lactate threshold (17, 18). Thus, it is clear that both high- and moderate-intensity exercise potentially induces mitochondrial fusion, but morphologic investigations combined with analyses of signaling events are lacking.

Therefore, the present study tested the hypothesis that both high- and moderate-intensity exercise induces mitochondrial fusion and associated signaling events. Moreover, it was hypothesized that fusion is more pronounced after high- compared with moderate-intensity exercise because of the higher energetic demand as well as the larger pool of recruited fibers. To test this hypothesis, transmission electron microscopy (TEM) and gene expression of important fusion and fission genes as well as protein content were determined in the muscles of swimmers completing exercise protocols with different metabolic demands.

MATERIALS AND METHODS

Subjects

Nine male swimmers (22.9 ± 0.9 yr of age) who had been enrolled in swimming competitions for at least 8 yr and in swimming training for at least 13 yr volunteered for the study. Their physical characteristics were as follows: weight, 78.9 ± 3.3 kg; height, 180.3 ± 1.7 cm; arm span, 186.6 ± 2.9 cm; maximal swimming speed of 2.0 ± 0.07 m/s; and best 100-m freestyle performance in a 25-m swimming pool of 53.6 ± 2.1 s. Additional detailed physical characteristics have been published elsewhere by Franco *et al.* (5). All subjects were fully informed of the risks and discomforts associated with the study, and all signed written informed consent. The study was conducted in accordance with the guidelines contained in the Declaration of Helsinki II and was approved by the Ethics Committee of the University of Granada (23/CEIH72015).

Experimental design

The full experimental design was recently published by Casuso *et al.* (19). In brief, we used a crossover study design in which each subject acted as his or her own control. All the interventions were made between 10:00 AM and 2:00 PM after a standardized light breakfast (40–55 g of whole wheat bread, 30–40 g of ham, and 250 ml of orange juice) consumed 2 h before the exercise. The study included 3 experimental days within a 2-wk period. Each experimental day was interspersed by 7 d, and the subjects were asked to refrain from physical activity for 48 h prior to each experimental day. During the first experimental day, we collected anthropometric data and resting muscle biopsies, which were considered as basal measurements (pretraining). During the next 2 d, after performing a standardized swimming warm-up (20), the subjects performed in a random order both high-intensity high-volume training (HIHVT) and sprint interval training (SIT) protocols, which were matched for total duration (~32–36 min). The SIT protocol consisted of 10 bouts of 50-m all-out effort every 4 min, whereas the HIHVT protocol consisted of 10 bouts of 200 m interspersed by 40-s intervals, during which they were asked to maintain the highest possible mean swimming speed throughout the total 2000 m. Immediately after each 50- or 200-m bout, heart rate (HR) was monitored using a Polar Team 2 (Bethpage, NY, USA), and a 6–20 rate of perceived exertion (RPE) scale was recorded. Blood lactate (Lactate Pro; Arkray, Kyoto, Japan) was measured at 3, 7, and 15 min postexercise, and the highest value within these time points was considered as lactate peak. After both protocols, muscle samples were collected 5 min upon exercise cessation (0 h). Afterwards, at 3 h postexercise, the procedure was repeated ~2 cm apart from the postexercise biopsy area.

Muscle samples

All skeletal muscle tissues were collected at a deepness of ~2–3 cm from the middle portion of the long head of the triceps brachii. Triceps brachii is a prime mover during the propulsive phase of front crawl swimming. In addition, triceps brachii exhibits a relatively glycolytic phenotype with lower mitochondrial volume than, for example, the often-sampled vastus lateralis. Therefore, potential mitochondrial morphology changes in response to exercise were assumed easier to observe. The biopsy procedure was performed while the subjects were lying face down. The skin, subcutaneous tissue, and fascia were anesthetized by injecting lidocaine at 2%. A muscle sample of ~20 mg was taken (16 g × 11 cm, CA1611; Coaxial Achieve; Merit Medical, South Jordan, UT, USA), and visible fat and blood were removed. A total of 3 punctures of ~8 mg each was obtained. Two of the samples were immediately frozen in liquid nitrogen and stored at −80°C until subsequent analysis, whereas another piece was prepared for TEM analysis (see TEM section).

Real-time quantitative PCR

We used the Real-Time Ready Custom Panel 96 (Roche, Basel, Switzerland), which is a 2-step real-time quantitative PCR platform. Briefly, total RNA was extracted from the triceps brachii using a PeqGold HP Total RNA Kit (VWR International, Randor, PA, USA) according to the manufacturer's recommendations. Isolated RNA was then treated with Turbo DNase (Thermo Fisher Scientific, Waltham, MA, USA). Final RNA concentration and quality were determined using a NanoDrop2000 (Thermo Fisher Scientific). cDNA was synthesized from total RNA using an iScript advanced cDNA Synthesis Kit (Bio-Rad, Hercules, CA, USA). The Real-Time Ready Custom Panel 96 (Roche) included the following specific primer pairs: MFN1 (125438; Roche), MFN2 (114631; Roche), fission, mitochondrial 1 (FIS1) (147077; Roche), mitochondrial fission factor (MFF) (148020; Roche), and parkin RBR E3 ubiquitin protein ligase (PARK2) (144556; Roche). The hypoxanthine phosphoribosyltransferase 1 (*HPRT1*) (102079; Roche), hydroxymethylbilane synthase (HMBS; 102110; Roche),

and β-actin (ACTB; 143636; Roche) genes were used as reference genes. These housekeeping genes were selected using the Minimum Information for Publication of Quantitative Real-Time PCR Experiments (MIQE; *http://www.rdml.org/miqe.php*) guidelines (21). The cDNA was then subjected to real-time quantitative PCR with the LightCycler 480 Probes Master Kit (Roche) on a LightCycler 480 Instrument II Detector (Roche). The PCR conditions were 1 cycle of 95°C for 10 min followed by 45 cycles of 95°C for 10 s, 60°C for 30 s, and 72°C for 1 s and 1 cycle of 40°C for 30 s. The expression level of each gene was analyzed with RT^2 Profiler PCR Array Data Analysis software (v.3.4; Qiagen, Germantown, MD, USA). Changes in gene expression were expressed as fold changes.

TEM

Muscle samples from 7 subjects were analyzed with TEM. Muscles were fixed with 2.5% (w/v) glutaraldehyde in 0.1 M cacodylate buffer for 6 h at 4°C and rinsed several times with 0.1 M cacodylate buffer. Samples were then postfixed with 1% osmium tetroxide for 1 h at room temperature, washed with 0.1 M cacodylate buffer, and treated with tannic acid at 0.15% for 1 min and then with uranyl acetate at 1% for 2 h at room temperature. The samples were dehydrated stepwise in ethanol concentrations (50, 70, and 90% for 20 min each and 2 steps in 100% for 15 min each). Samples were then incubated with ethanol propylene oxide 1:1 for 15 min and 1:1 propylene oxide resin for 4 h in agitation at room temperature and transferred to 100% epoxy resin overnight. Subsequently, they were embedded in fresh epoxy resin and left in the oven at 60°C for 48 h to polymerize. Ultrathin sections (60 nm) were prepared using a diamond knife (Diatome, Hatfield, PA, USA) and contrasted with double stain with uranyl acetate and lead citrate prior to examination with an LEO 906E transmission electron microscope (Carl Zeiss, Oberkochen, Germany). Images were taken at ×10,000 magnification. From each subject, we analyzed 5 images for each time point and for each cell-region both from transversal and longitudinal cuts.

Mitochondrial shape descriptors and size measurements were obtained for subsarcolemmal (SS) and IMF mitochondria on TEM micrographs from longitudinal and transversal planes. SS mitochondria were defined as structures concentrated under the sarcolemma and sometimes close to the peripherally located myonuclei. In contrast, IMF mitochondria were defined as those located between myofibrils. In this step, we used ImageJ (v.1.51a; National Institutes of Health, Bethesda, MD, USA; *http://rsb.info.nih.gov/ij*) by manually tracing clearly discernible outlines of mitochondria as previously described by Picard *et al*. (22). Surface area (or mitochondrial size) is reported in square micrometers; perimeter is reported in micrometers. We determined 2 different characteristics: aspect ratio (AR), which was computed as [(major axis)/(minor axis)] and reflects the length-to-width ratio, and form factor (FF), which is computed as $[(\text{perimeter}^2)/(4\pi \cdot \text{surface area})]$ and reveals the complexity and branching aspect of mitochondria (23).

In addition, we used the same micrographs used to analyze mitochondrial morphology to quantify glycogen content. For that purpose, we modified the protocol used by Nielsen *et al.* (24) for ultrathin sections (60 nm). We manually traced the glycogen surface, and then the area of selection was calculated in square pixels (area). Subsequently, we quantified the mean gray value within the selection. This is the sum of the gray values of all the pixels in the selection divided by the number of pixels. Glycogen in a given micrograph was quantified as mean/area.

Mitochondrial volume density

We used the 2-tier point counting protocol in order to estimate mitochondrial volume density ($Mito_{VD}$) (25). A grid (420 × 420 nm) was overlapped to the electron micrographs (×10,000 magnification), and the ratio of the number of points that fall on the mitochondria to the number of points that fall on the entire area was calculated (25). $Mito_{VD}$ was expressed as the relative percentage to the total cell area.

Western blotting

Triceps brachii samples were harvested in 10 mM Tris-HCl (pH 7.5), 150 mM NaCl, 2 mM EDTA, 1% Triton X-100, 10% glycerol, and a protease inhibitor cocktail (Thermo Fisher Scientific) and were placed on ice for 20 min. After centrifugation (30 min, 13,000 *g*, 4°C), the protein content in the supernatant was determined using a Protein Assay Kit II (Bio-Rad). Samples containing 30 μg of protein were mixed with 3× SDS-PAGE sample buffer [100 mM Tris-HCl (pH 6.8), 25% SDS, 0.4% bromophenol blue, 10% 2-ß-mercaptoethanol, and 2% glycerol], separated *via* SDS-PAGE using Any kD TGX Gel (Bio-Rad), and transferred onto a nitrocellulose membrane (Bio-Rad). After incubation in blocking buffer (5% nonfat milk and 1% Tween 20 in Tris-buffered saline), the membranes were probed with the following antibodies: rabbit anti-MFN2 (D2D10) (1:1000 in 5% nonfat milk) antibody (482S) acquired from Cell Signaling Technology (Leiden, The Netherlands), mouse anti-OPA1 antibody (612606; 1:1000 in 5% nonfat milk) acquired from BD Biosciences (Franklin Lakes, NJ, USA), mouse anti-FIS1 antibody (sc-376447; 1:200 in 5% nonfat milk) acquired from Santa Cruz Biotechnology (Dallas, TX, USA), anti–heat shock protein 70 (Hsp-70) (sc-7298; internal control; 1:500 in 5% nonfat milk) acquired from Santa Cruz Biotechnology, and anti-membrane-associated ring finger (C3HC4) 5 (MARCH5) (ab77585; 1:500 in 5% bovine serum albumin) acquired from Abcam (Cambridge, United Kingdom). Hsp-70 was used as an internal control because it showed better stability than β-actin and tubulin (Supplemental Fig. S1). Immunoreactive signals were detected *via* ECL (SuperSignal West Dura Chemiluminescent Substrate, 34075; Thermo Fisher Scientific), and the membranes were digitally imaged and quantified through densitometry using ImageJ software. The results are represented as the fold-change in expression relative to pretraining levels.

Statistical analysis

Statistical analyses were performed using SPSS v.22 (IBM SPSS, Chicago, IL, USA) for Windows. Data are represented as the means ± SD. Normality was checked through Kolmogorov-Smirnov tests. Significant differences in gene expression, protein levels, and mitochondrial morphology changes were assessed using ANOVA with repeated measures. Bonferroni correction was applied in a *post hoc* pairwise comparison. In addition, Pearson regression analysis was performed between AR and FF for each time point (pretraining, 3 h, and posttraining). In order to compare the different time points, slopes of the respective curves were compared by ANCOVA. The statistical comparison of the slopes was performed using Statistica v.7.1 (StatSoft, Tulsa, OK, USA). Statistical significance was defined as $P < 0.05$.

TABLE 1. *Protocol data*

Variable	SIT	HIHVT
HR (bpm)	172 ± 7.9	175 ± 8.1
RPE (6–20 scale)	17.4 ± 2.7***	14.8 ± 3.5
Velocity (m/s)	1.74 ± 0.09***	1.30 ± 0.07
Lactate peak (mM)	13.8 ± 0.3***	9.4 ± 0.8

HR of RPE and velocity is presented as the mean of each bout. Lactate peak was considered as the higher value recorded within 15 min after the end of each protocol. Means ± SD. ***$P < 0.001$.

TABLE 2. $Mito_{VD}$

Variable	Pretraining	SIT posttraining	SIT 3 h	HIHVT posttraining	HIHVT 3 h
IMF $Mito_{VD}$ (%)	5.00 ± 0.27	5.65 ± 1.4	3.77 ± 0.59*	5.13 ± 1.03	5.60 ± 0.66
SS $Mito_{VD}$ (%)	3.66 ± 0.47	3.40 ± 0.67	3.62 ± 0.39	3.29 ± 1.62	3.88 ± 2.01

Values are means ± SD. IMF, IMF mitochondria; SS, SS mitochondria. *$P < 0.05$ *vs.* pretraining.

RESULTS

Detailed information regarding the protocol data has been previously published elsewhere by Casuso *et al.* (19). In brief, the SIT protocol (~1.74 m/s) was performed at a higher mean speed than the HIHVT protocol (~1.30 m/s) (**Table 1**). However, mean maximal HR was similar between both protocols (172 ± 7.9 bpm and 175 ± 8.1 bpm for SIT and HIHVT, respectively). On the other hand, the 6–20 RPE scale (17.4 *vs.* 14.8) and peak blood lactate (13.8 *vs.* 9.4 mM) were higher in SIT than for HIHVT. $Mito_{VD}$ (**Table 2**) was 5.00 ± 0.27% for IMF mitochondria and 3.66 ± 0.47% for SS mitochondria at rest (Table 2). $Mito_{VD}$ in response to exercise is further described in Table 2.

Figure 1 shows representative TEM micrographs for mitochondrial analysis. TEM images reveal fragments of the mitochondrial reticulum, but we will use the term "mitochondria" for simplicity. First, we quantified AR and

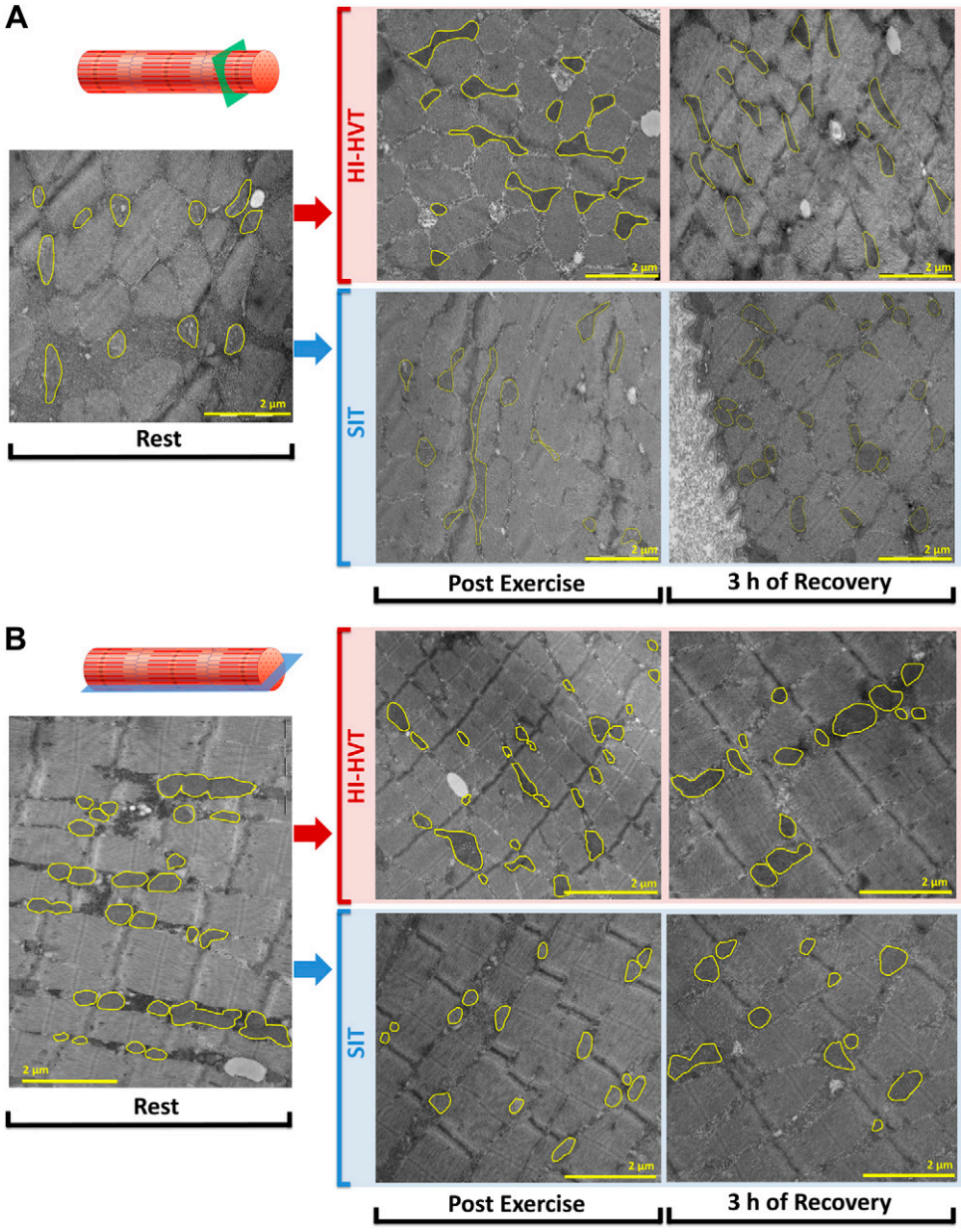

Figure 1. Representative micrographs of mitochondrial morphology from the same subject. Transversal (*A*) and longitudinal (*B*) cut. Scale bars, 2 μm.

FF (**Fig. 2**). As mentioned above, AR reflects the length-to-width ratio, whereas FF reveals the complexity and branching aspect of mitochondria (22). SIT significantly increased the branching complexity of IMF mitochondria when analyzed in the transversal plane (Fig. 2*A*), but no other significant effect was found in response to SIT (Fig. 2*B–D*). When analyzing transversal cuts from HIHVT, we found that both IMF and SS mitochondria increased their branched complexity posttraining and 3 h after training (Fig. 2*E, G*). In addition, when analyzing longitudinal cuts, our results showed that SS mitochondria increased their branched complexity, but this effect was only evident after 3 h (Fig. 2*H*).

Then, we analyzed markers of mitochondrial size, including area and perimeter (**Fig. 3**). Mitochondrial area (μm^2) and perimeter (μm) were similar between IMF ($0.13 \pm 0.082\ \mu m^2$; $1.39 \pm 0.60\ \mu m$) and SS ($0.16 \pm 0.11\ \mu m^2$; $1.50 \pm 0.64\ \mu m$) at rest (Fig. 3*A, B*). Both IMF ($0.15 \pm 0.09\ \mu m^2$; $1.50 \pm 0.72\ \mu m$; $P < 0.05$) and SS ($0.20 \pm 0.13\ \mu m^2$; $1.64 \pm 0.71\ \mu m$; $P < 0.05$) mitochondrial size increased post-SIT. In addition,

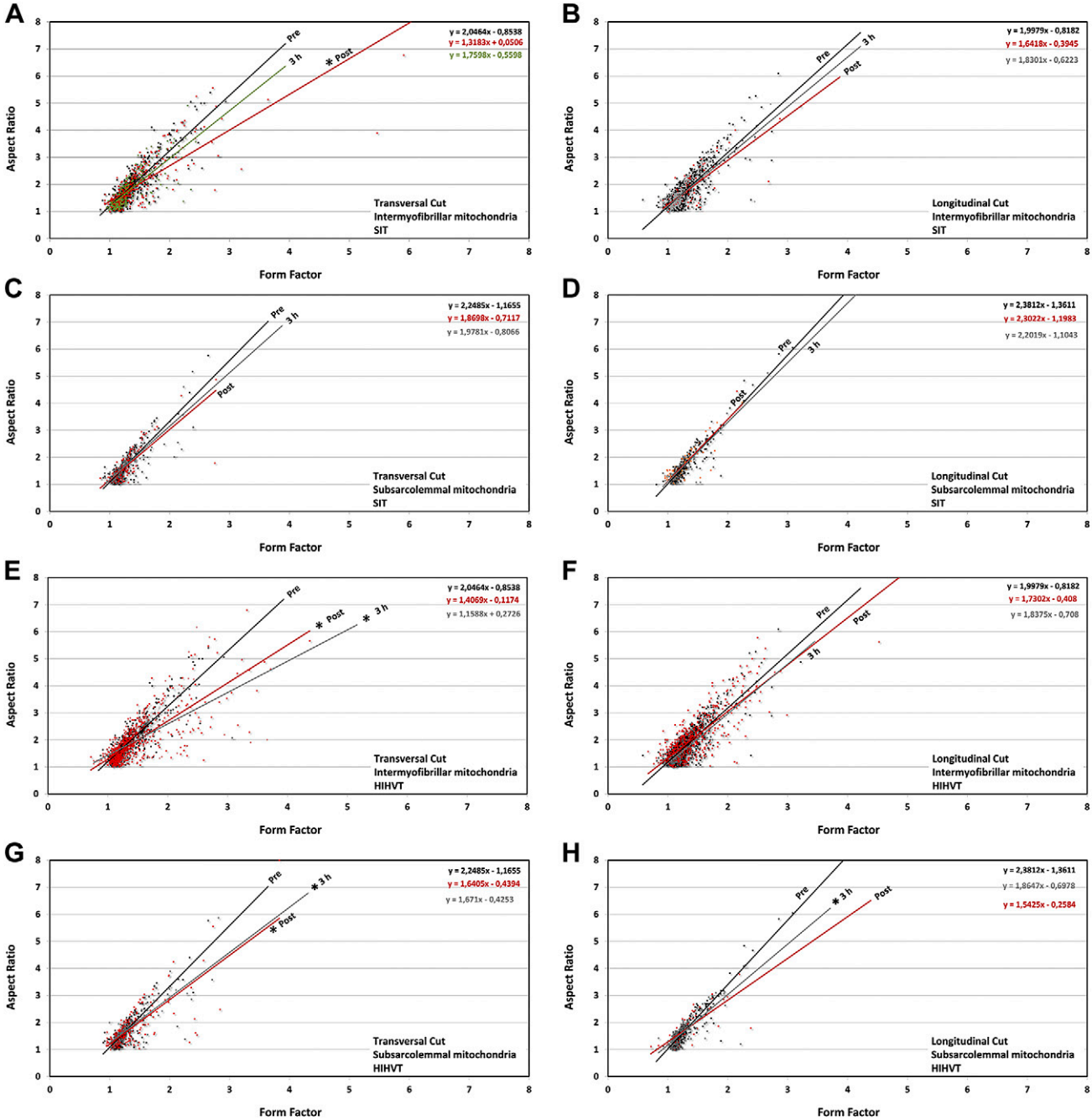

Figure 2. FF and AR in SS and IMF mitochondria in the transverse and longitudinal planes. *A–D*) The FF/AR distribution in response to SIT separated by IMF and SS fractions and considering the transverse and longitudinal planes. *E–H*) The FF-AR distribution in response to HIHVT separated by IMF and SS fractions and considering the transverse and longitudinal planes. $*P < 0.05$, $***P < 0.001$ denote different slope to pretraining. Note that the results are from 7 subjects and that we manually traced well-visualized mitochondria.

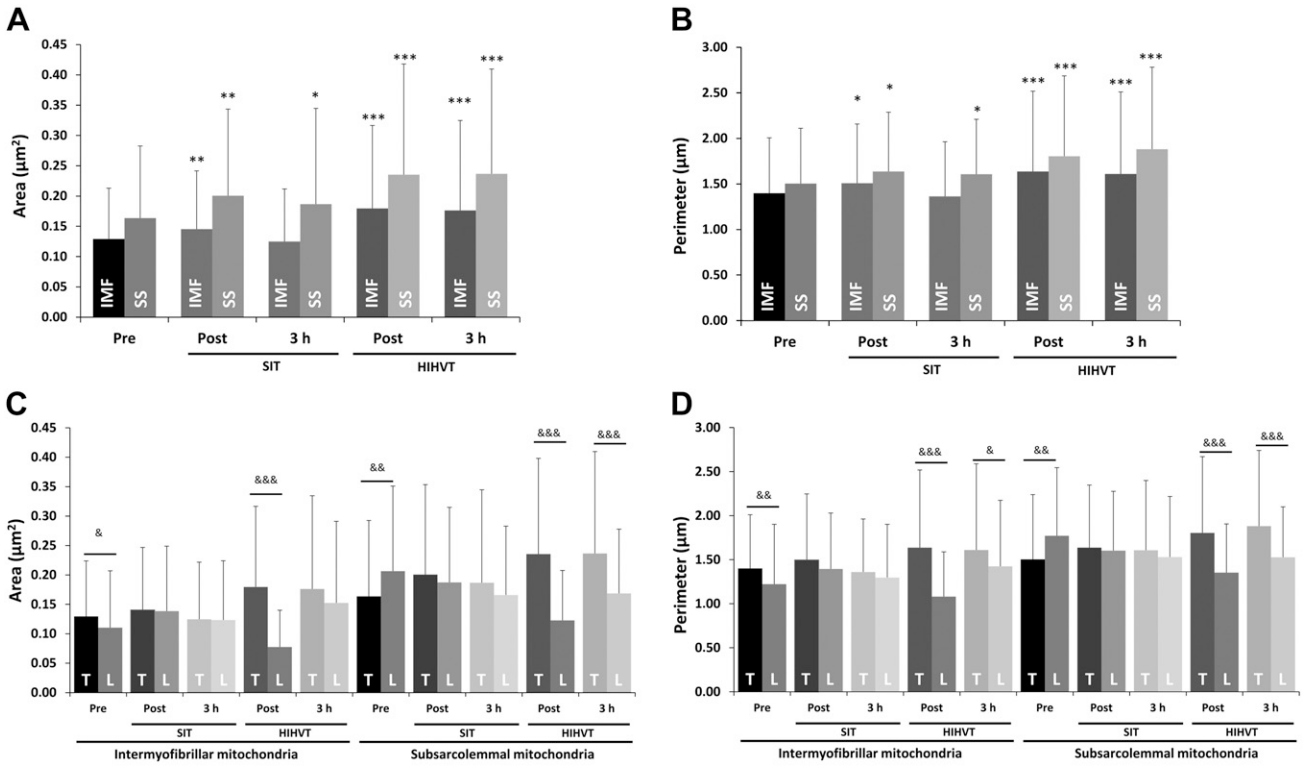

Figure 3. Areas and perimeters in SS and IMF mitochondria from the transverse and longitudinal planes. *A*, *B*) Area (*A*) and perimeter (*B*) of IMF and SS mitochondria. *C*, *D*) Area (*C*) and perimeter (*D*) of IMF and SS mitochondria in the transversal and longitudinal planes. Data are means ± SD. $^{*}P < 0.05$, $^{**}P < 0.01$, $^{***}P < 0.001$ compared with pretraining; $^{\&}P < 0.05$, $^{\&\&}P < 0.01$, $^{\&\&\&}P < 0.001$ compared with the transversal and longitudinal planes. L, longitudinal plane; T, transversal plane.

3 h after SIT, SS (0.19 ± 0.15 μm²; 1.61 ± 0.80 μm; $P < 0.05$) but not IMF (0.12 ± 0.08 μm²; 1.36 ± 0.60 μm) mitochondrial size remained higher if compared with pretraining levels. In regard to HIHVT, both IMF (0.18 ± 0.13 μm²; 1.64 ± 0.88 μm; $P < 0.001$) and SS (0.24 ± 0.18 μm²; 1.81 ± 0.96 μm; $P < 0.001$) mitochondrial size increased postexercise. This effect was maintained 3 h postexercise for IMF (0.18 ± 0.14 μm²; 1.61 ± 0.90 μm; $P < 0.001$) and SS (0.24 ± 0.17 μm²; 1.88 ± 0.86 μm; $P < 0.001$) mitochondria.

We then analyzed the mitochondrial morphology from the longitudinal and transversal planes (Fig. 3*C*, *D*). IMF mitochondria at rest were higher ($P < 0.05$) in the transversal (0.13 ± 0.09 μm²; 1.40 ± 0.60 μm, $n = 429$) than the longitudinal plane (0.11 ± 0.09 μm²; 1.22 ± 0.67 μm, $n = 697$). Post-SIT, there were no changes in IMF when comparing mitochondrial size from the transversal (0.14 ± 0.10 μm²; 1.50 ± 0.74 μm, $n = 376$) and from the longitudinal plane (0.14 ± 0.11 μm²; 1.39 ± 0.63 μm, $n = 106$). This effect was maintained 3 h post-SIT both in the transversal (0.12 ± 0.09 μm²; 1.36 ± 0.60 μm, $n = 215$) and longitudinal plane (0.12 ± 0.10 μm²; 1.30 ± 0.61 μm, $n = 331$). In contrast to SIT, we observed that, post-HIHVT, IMF mitochondria were higher ($P < 0.001$) when analyzed from the transversal (0.23 ± 0.16 μm²; 1.80 ± 0.86 μm, $n = 268$) than from the longitudinal plane (0.12 ± 0.08 μm²; 1.35 ± 0.57 μm, $n = 56$). Moreover, IMF mitochondria perimeter was still higher 3 h post-HIHVT ($P < 0.05$) from the transversal (1.88 ± 0.82 μm, $n = 117$) than from the longitudinal plane (1.53 ± 0.57 μm, $n = 240$), whereas no difference was found between transversal area (0.24 ± 0.17 μm², $n = 117$) and longitudinal area (0.17 ± 0.10 μm², $n = 240$).

In contrast to IMF, the SS mitochondria at rest were higher ($P < 0.01$) in the longitudinal (0.21 ± 0.13 μm²; 1.77 ± 0.69 μm, $n = 161$) than the transversal plane (0.16 ± 0.12 μm²; 1.50 ± 0.71 μm, $n = 173$). We found that, post-SIT, SS mitochondrial size was similar when observed from the longitudinal (0.19 ± 0.12 μm²; 1.60 ± 0.67 μm, $n = 143$) and transversal plane (0.20 ± 0.15 μm²; 1.64 ± 0.71 μm, $n = 184$). This effect was maintained 3 h after SIT because mitochondrial size was similar between longitudinal (0.17 ± 0.12 μm²; 1.53 ± 0.68 μm, $n = 133$) and transversal planes (0.19 ± 0.16 μm²; 1.60 ± 0.74 μm, $n = 131$). Notably, post-HIHVT a greater ($P < 0.001$) SS mitochondrial size existed in the transversal (0.24 ± 0.16 μm²; 1.81 ± 0.83 μm, $n = 268$) than the longitudinal plane (0.12 ± 0.08 μm²; 1.35 ± 0.52 μm, $n = 56$). Moreover, 3 h post-HIHVT the SS mitochondrial size was still higher ($P < 0.001$) from a transversal (0.24 ± 0.17 μm²; 1.88 ± 0.85 μm, $n = 117$) than from a longitudinal plane (0.16 ± 0.10 μm²; 1.52 ± 0.57 μm, $n = 240$).

Figure 4 shows representative TEM micrographs for glycogen analysis. We quantified glycogen (mean/area) in the SS and IMF subcellular compartments (**Fig. 5**). IMF glycogen content decreased post-SIT (1490 ± 1236; $P < 0.05$) when compared with glycogen content at rest (1665 ± 1525) and remained low after 3 h of rest (1010 ± 818; $P < 0.001$). Notably, IMF glycogen was not reduced post-HIHVT (1620 2± 1305) nor 3 h after HIHVT (1598 ± 1261). When looking at SS glycogen, our results show that, if compared

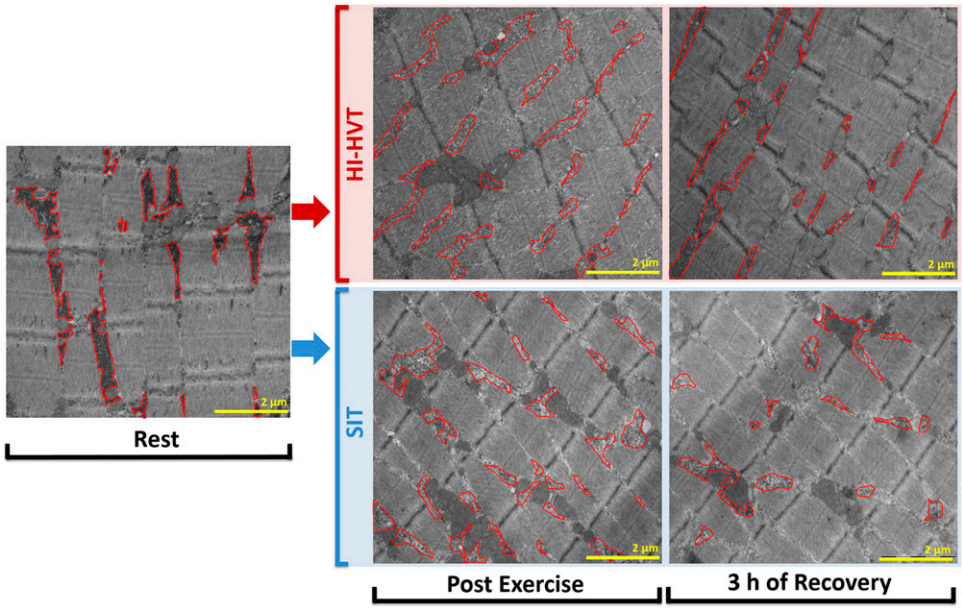

Figure 4. Representative micrographs of glycogen quantification from the same subject. Scale bars, 2 μm.

with the rest levels (1654 ± 1682), both SIT (658 ± 526) and HIHVT (590 ± 673) decreased glycogen content posttraining ($P < 0.001$). However, at 3 h posttraining, glycogen began to increase in response to HIHVT (1005 ± 1070), whereas the mean/area remained low in response to SIT (335 ± 298; $P < 0.01$ compared with HIHVT).

An analysis of mRNA levels of key proteins involved in mitochondrial fusion (MFN1 and MFN2) and in mitochondrial fission and mitophagy (FIS1, MFF, and PARK2) is shown in **Fig. 6**. MFN1 ($P < 0.01$, Fig. 6*A*) and MFN2 ($P < 0.001$, Fig. 6*B*) were induced posttraining in response to SIT, whereas no changes were detectable after HIHVT. Indeed, we found that posttraining MFN1 and MFN2 mRNA levels were higher ($P < 0.05$) for SIT than for HIHVT. Moreover, SIT induced an increase in FIS1 mRNA levels at 0 h ($P < 0.05$). Notably, FIS1 mRNA (Fig. 6*C*) levels in response to HIHVT compared with SIT were lower both at 0 h ($P < 0.05$) and at 3 h ($P < 0.05$). MFF mRNA levels decreased ($P < 0.05$) posttraining in response to both SIT and HIHVT (Fig. 6*D*). Importantly, MFF expression was higher 3 h post-SIT than 3 h post-HIHVT. The expression of PARK2 mRNA decreased ($P < 0.05$) after HIHVT, and no other changes were evident (Fig. 6*E*). Accordingly, no authophagosome-like structures were identified in TEM images, suggesting that, under our experimental conditions, more time may be needed in order to stimulate mitophagy. Therefore, we next explored MARCH5 protein content because it triggers PARK2 recruitment to damaged mitochondria (26). However, MARCH5 protein content was not altered after exercise (Supplemental Fig. S2). These results are in accordance with recent observations showing that acute exercise does not increase the mitophagic flux in well-trained subjects (27).

Finally, we assessed MFN2, OPA1, and FIS1 protein expression (**Fig. 7**). We found that MFN2 was increased at 3 h in response to both HIHVT and SIT ($P < 0.05$) compared with both pre- and posttraining levels. Notably, OPA1 increased rapidly in response to HIHVT and remained higher at 3 h posttraining ($P < 0.05$). In addition, we found that, at 3 h post-OPA1, expression was higher for HIHVT than for SIT ($P < 0.05$). Notably, FIS1 numerically increased several times in response to HIHVT ($n = 6$). However, no statistically significant effect of exercise was apparent. A full uncut blot is provided in Supplemental Fig. S1.

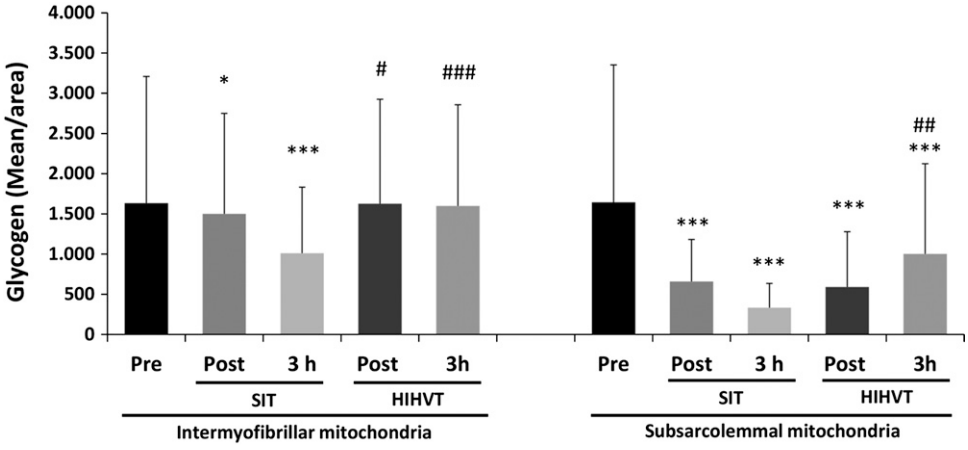

Figure 5. Glycogen content quantified from the same micrographs used for mitochondrial morphology analysis ($n = 7$ subjects). Data are means ± SD. $^{*}P < 0.05$, $^{***}P < 0.001$ compared with pretraining; $^{\#}P < 0.05$, $^{\#\#}P < 0.01$, $^{\#\#\#}P < 0.001$ compared with SIT at the same time point.

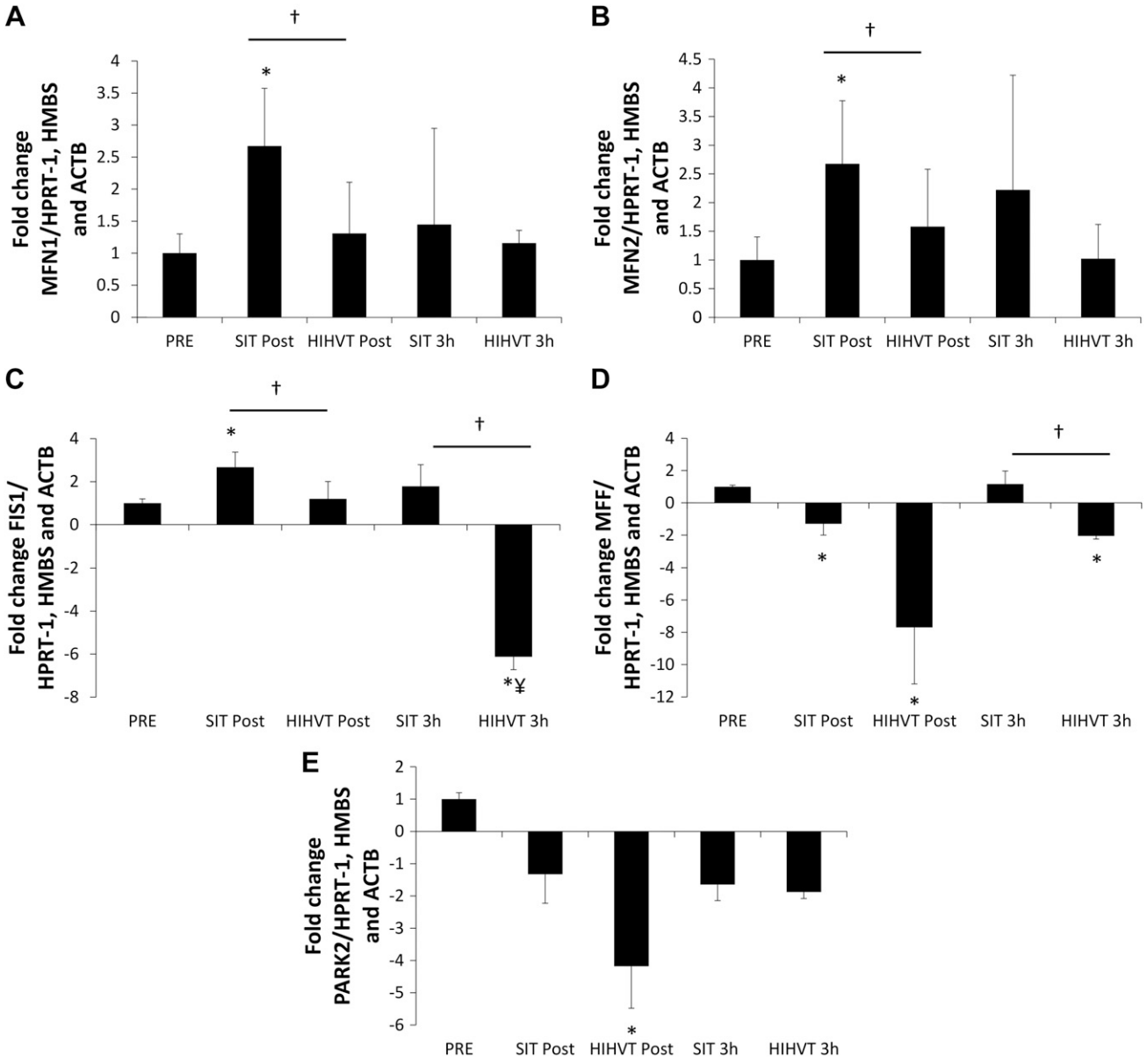

Figure 6. Expression of genes related to mitochondrial fusion, fission, and mitophagy. *A*, *B*) MFN1 (*A*) and MFN2 (*B*) were analyzed as markers of mitochondrial fusion. *C*, *D*) FIS 1 (*C*) and MFF (*D*) were analyzed as markers of mitochondrial fission. *E*) Park2 was analyzed as a marker of mitophagy. HPRT, hypoxanthine phosphoribosyltransferase. Data are means ± SD. $^{*}P < 0.05$ *vs.* pretraining; $^{\dagger}P < 0.05$ SIT *vs.* HIHVT; $^{¥}P < 0.05$ posttraining *vs.* 3 h.

DISCUSSION

Mitochondrial morphology changes can be induced within a few minutes (28). The present study reveals that high-intensity exercise induces changes in mitochondrial morphology suggestive of increased mitochondrial fusion within the skeletal muscle of well-trained athletes. Additionally, the applied exercise protocol and associated differences in metabolism appear to be of importance for the degree of mitochondrial morphology changes. This is of importance because the time course for changes of mitochondrial morphology in response to exercise is relatively unknown. Indeed, mitochondrial dynamics during and after exercise have mainly been analyzed at the molecular level.

Protein regulation and signaling occur within minutes during and following skeletal muscle contraction. For example, a single bout of exercise induces a rapid increase of PGC-1α protein content in human skeletal muscle (29). Moreover, PGC-1α translocation to the nucleus (17) and estrogen-related receptor (ERR)-α expression occur within 2 h (16). Notably, the initial increase of peroxisome proliferator-activated receptor-γ coactivator (PGC)-1α and ERR-α transcription appears to induce the expression of MFN2 (16). Accordingly, both continuous moderate-intensity and sprint exercise are associated with rapidly elevated MFN2 mRNA levels after exercise (17, 18). Similarly, when highly trained subjects are submitted to strenuous continuous exercise, both MFN1 and MFN2 mRNA levels increase for 24 h (16). These

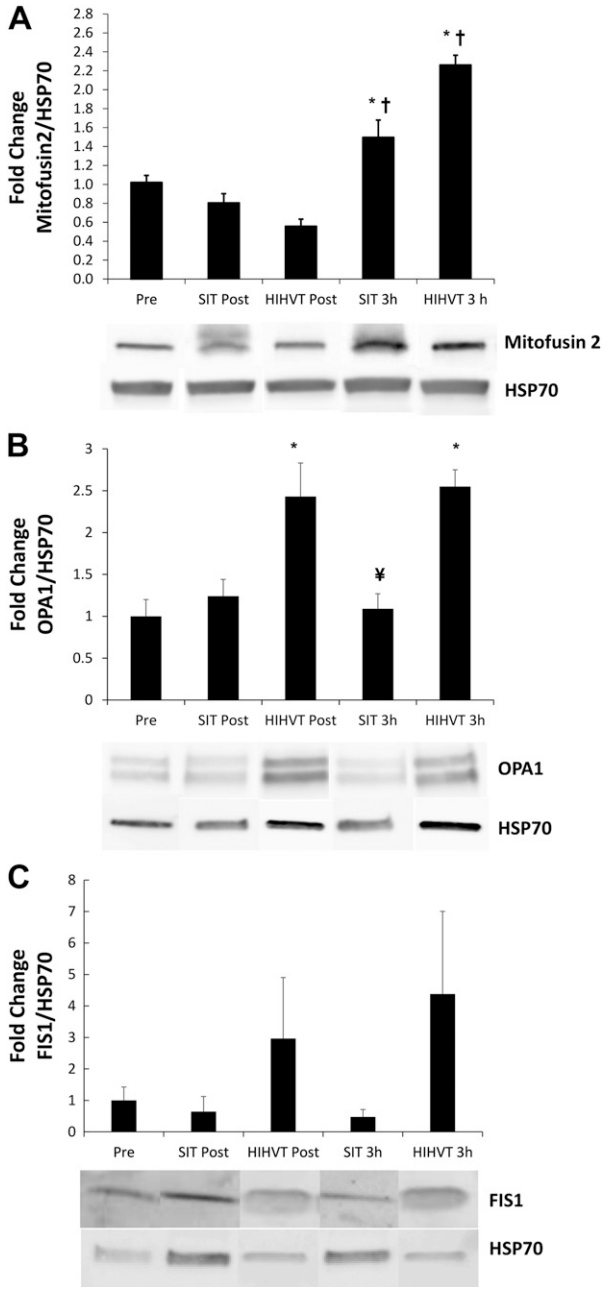

Figure 7. MFN2 (*A*), OPA1 (*B*), and FIS1 (*C*) protein content. Hsp-70 was used as a loading control. Note that FIS1 data are from 6 subjects. Images are cut from different membranes. Data are means ± SD. $^{*}P < 0.05$ compared with pretraining; $^{\dagger}P < 0.05$ compared with posttraining; $^{¥}P < 0.05$ SIT *vs.* HIHVT.

studies are in accordance with our results showing that SIT increases MFN1 and MFN2 mRNA levels. However, we failed to detect these mRNA changes in response to HIHVT, whereas MFN2 protein increased 3 h after HIHVT. This suggests that MFN mRNA peak levels may differ between SIT and HIHVT.

Surprisingly, the present results show that the increased MFN2 protein expression following HIHVT is even higher than the changes previously observed after 4–6 wk of training (8, 30). In addition, Cartoni *et al.* (16) did not observe changes in MFN2 protein content for 24 h after continuous strenuous exercise. These discrepancies could be related to the investigated muscle group. The triceps brachii exhibits a higher fraction of glycolytic (*i.e.*, type IIa and IIx) fibers than the vastus lateralis (31), which likely contributes to the lower maximal mitochondrial respiration (32) and β-oxidation (33) observed in arm compared with leg musculature. Moreover, the triceps brachii, in contrast to the vastus lateralis, appears less adaptable to intense exercise as judged by citrate synthase expression changes (31, 34). Our data suggest that the triceps brachii has adapted to rapidly change its mitochondrial morphology in response to cellular energetic drops, which may help to distribute energy through the muscle cell (11, 12). In addition to the studied muscle, it should be highlighted that our data are from swimmer athletes. Well-trained skeletal muscle shows a high mitochondrial content and a high level of PGC-1α. This likely contributes to the increased profusion environment and the expanded tubular mitochondrial network observed in response to an exercise training regimen (35, 36). Moreover, the higher MFN2 content within trained skeletal muscle (8) may help to rise the fusion events during exercise in athletes.

It should, however, be noted that MFN2 is not mitochondria-specific, and it can also be found in the sarcoplasmic reticulum (37). In contrast, OPA1 is found in the inner mitochondrial membrane and has several isoforms. The short isoforms regulate mitochondrial supercomplex formation, whereas the long isoforms are essential for mitochondrial fusion (38, 39). However, both long and short isoforms are required to maintain a dynamic mitochondrion (39). Therefore, in spite of similar MFN2 expression between protocols, our results suggest that mitochondrial morphology changes differ between SIT and HIHVT. In fact, the observation of a robust OPA1 expression suggests that mitochondrial morphology changes are compatible with inner mitochondrial membrane fusion in response to HIHVT.

Another process that can induce mitochondrial morphology changes is fission, which consists in the fragmentation of damaged or dysfunctional mitochondria. In humans, SIT increases leg mitochondrial respiration without an increment in mitochondrial content (30), which could be explained by an improvement of mitochondrial function through eliminating defective organelles by fission and mitophagy (40). Our results show that SIT induced a raise in the mRNA levels of FIS1, which, indeed, was higher than HIHVT. Moreover, our results show that SIT also increased MFF expression if compared with HIHVT. Importantly, MFF is the main receptor by which dynamin-related protein (DRP)-1 is recruited from the cytosol to the damaged mitochondria in response to cellular energy drops (41, 42). In addition, FIS1 constitutes an alternative pathway to MFF as a receptor of the DRP-1 pathway (3, 43). Indeed, FIS1 overexpression is known to increase mitochondrial fragmentation (44, 45). This may suggest that our SIT protocol may stimulate mitochondrial quality control through these 2 mitochondrial DRP-1 receptors to a higher extent than HIHVT. It should be noted that the time point expression of the genes and proteins explored here has not been studied in detail in exercised human skeletal muscle, and some of them may require more time to be expressed. As an example, we observed

SIT to induce an increased FIS1 mRNA expression, but, as noted in Fig. 7, more than 3 h may be needed in order to detect an associated increase of FIS1 protein expression. However, in the present study, it must be noted a numerical nonsignificant increase in FIS1 protein content was present in response to HIHVT. Thus, the possibility of a FIS1-mediated mitochondrial fission in some subjects after HIHVT remains and should be investigated further.

Collectively, the data suggest that SIT and HIHVT differ in the underlying molecular mechanisms as well as in the duration of the mitochondrial morphologic changes. We found that SIT induced a reduction of both IMF and SS glycogen, whereas HIHVT only reduced SS glycogen. Notably, glycogen content remained low 3 h after SIT. This is in accordance with a previous study showing that arm skeletal muscle glycogen content is still low 4 h after strenuous exercise (46). Moreover, the fact that SIT significantly depletes IMF glycogen whereas HIHVT does not is in line with the fact that sprint exercise dramatically increases cellular energy demands (13, 14, 47). Accordingly, data from the SIT protocol match the "power transmitting cables theory" proposed by Skulachev (11), which suggests that IMF mitochondria undergo fusion in order to energetically interconnect the sarcolemma and core of the muscle cell. Notably, we found that mitochondrial morphology changes were higher immediately after SIT, and all of these markers returned to basal levels after 3 h. This morphologic change might facilitate energy distribution from oxygen-rich areas, which are close to the sarcolemma, to deeper areas with oxygen deficits. Accordingly, it has been described that SS mitochondria show a greater trainability than IMF mitochondria. In fact, SS $Mito_{VD}$ is ~0.15% in untrained subjects, which can increase up to ~3.5%; whereas IMF $Mito_{VD}$ is ~4% in untrained subjects and can rise up to ~7.5% (48). Therefore, skeletal muscle may adapt to enhance energy delivery to the core of the muscle cell at high exercise intensities (49). It should, however, be noted that, in response to SIT, some fission markers are also elevated. Thus, it is possible that SIT-induced mitochondrial morphology changes reflect both fission and fusion events.

In response to HIHVT, the microscopy data, together with a lack of expression of MFF and FIS1 and the increment in MFN2 and OPA1 protein content, likely suggest that the mitochondrial morphologic changes suggest an increased fusion. It is important to note that, at rest, SS mitochondrial size is greater in the longitudinal plane than in the transversal plane (Fig. 3*C, D*). This distribution is changed after HIHVT, when mitochondrial areas and perimeters are greater in the transversal plane than in the

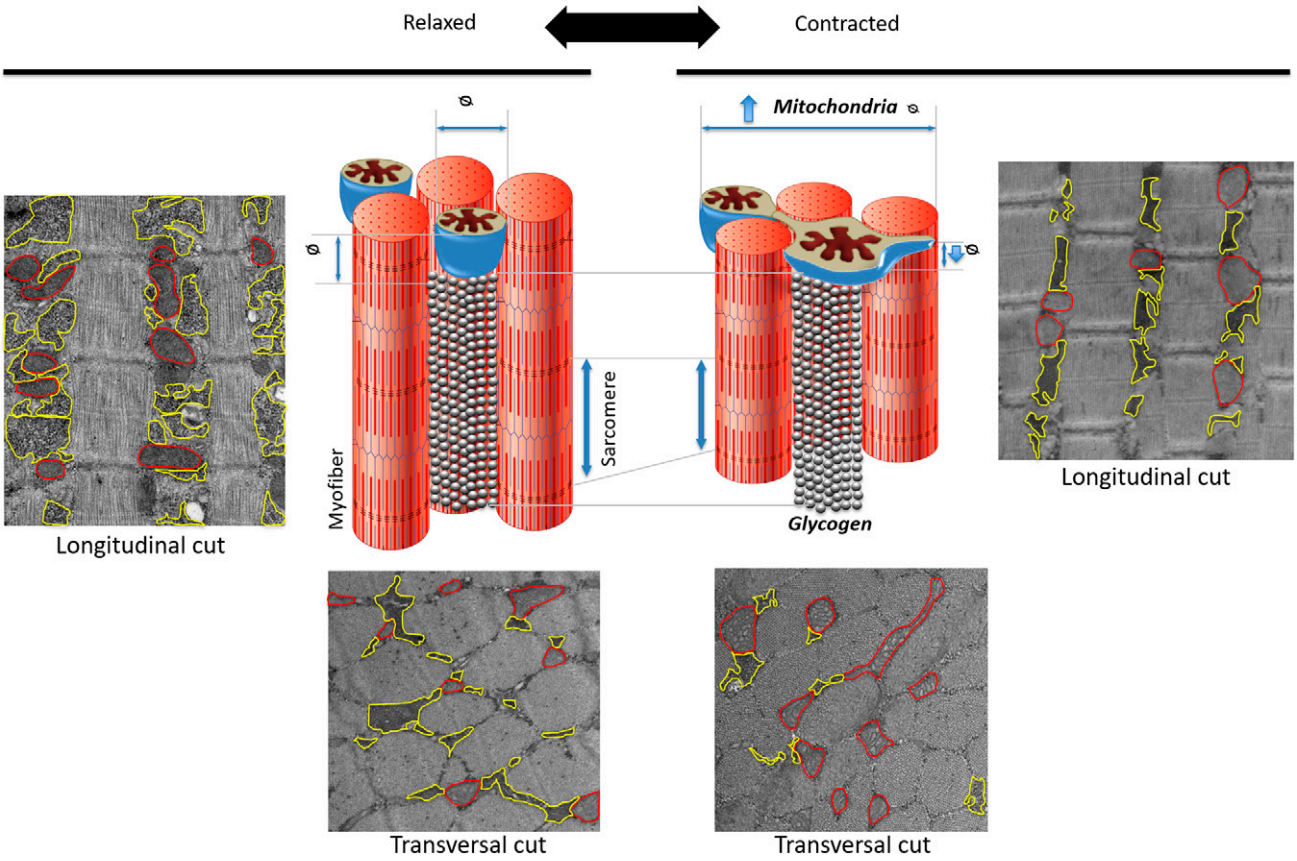

Figure 8. Theoretical representation of flattened mitochondria between contracting myofibrils during HIHVT. Skeletal muscle mitochondria are packed between myofibrils, and, as proposed in the right side of the picture, contracting myofibrils can squeeze mitochondria. Additionally, during HIHVT, the IMF glycogen is not depleted. Therefore, it can exert additional pressure to mitochondria. This might explain why, in response to HIHVT, mitochondrial fusion mainly occurs in one orientation. The micrographs are taken from the same subject at pretraining (left cuts) and posttraining (right cuts). Mitochondria and glycogen are traced in red and yellow, respectively.

longitudinal plane (Fig. 3*C*, *D*). To our knowledge, there are no previous findings reporting mitochondrial morphologic changes in different orientations in response to exercise. Nevertheless, it has been recently reported that mechanical forces can promote mitochondrial morphology changes leading to fragmentation (2, 50). The fact that we observed a down-regulation of FIS1 and MFF gene expression led to the hypothesis that mitochondrial morphologic changes in response to HIHVT may occur in response to intramuscular forces by which mitochondria are getting squashed between muscle fibers. In addition, it can be speculated that intramuscular glycogen may help increase intracellular strain within contracting muscles during HIHVT (theoretically explained in **Fig. 8**). However, further mechanistic studies are needed to assess whether intramuscular forces may trigger mitochondrial morphologic changes suggestive of fusion in response to exercise.

The main strength of the study is that we analyzed mitochondrial fusion within well-adapted skeletal muscle in response to intense exercise at both the molecular and morphologic levels. Even though it can be discussed that the TEM analysis of 7 out of 9 subjects limits the results of the study, it has been confirmed that mitochondrial morphologic changes occurred in athletes during high-intensity exercise. In this context, it should be mentioned that mitochondrial morphology quantification by TEM has been a matter of discussion for years. Gollnick and King (51) observed that rats submitted to strenuous exercise showed an aberrant mitochondrial swelling and cristae disorganization. However, these effects were later attributed to the method of fixation (52), which is decisive when quantifying mitochondrial morphology. The method used in the present study (*i.e.*, fixing in glutaraldehyde and then postfixing in osmium) seems to properly characterize postexercise mitochondrial function (52, 53), but it cannot be excluded that artifacts exists. Finally, the lack of control subjects (*i.e.*, sedentary or less-trained subjects) limits the conclusions of the study.

CONCLUSIONS

Mitochondrial morphologic changes suggestive of fusion occur in well-adapted human skeletal muscle during high-intensity exercise. Moreover, HIHVT induces longer mitochondrial morphology changes and higher OPA1 protein expression than SIT. Although this may suggest a different degree of mitochondrial fusion, further mechanistic studies should evaluate the effects of exercise volume and intensity on acute mitochondrial dynamics. FJ

ACKNOWLEDGMENTS

The authors thank Daniel Camiletti Moirón (University of Cádiz, Cádiz, Spain) and Jerónimo Aragón-Vela (University of Granada) for technical assistance, and Mohamed Tassi Mzanzi (University of Granada) for helpful comments on transmission electron microscopy analysis. F.J.R.-O. and J.P.-D. are part of the University of Granada Plan Propio de Investigación 2016. This study was partially supported by Grant SAF2015-65786-R from the Ministerio de Economía y Competitividad, Grant 3650 managed by Fundación General Empresa–Universidad de Granada, and the CTS-454 investigation group, "Impacto Fisiologico del estres Oxidativo, Deporte, Actividad Física y Salud." The authors declare no conflicts of interest.

AUTHOR CONTRIBUTIONS

J. R. Huertas and R. A. Casuso designed the study, interpreted the data, and wrote the manuscript; F. J. Ruiz-Ojeda and J. Plaza-Díaz were involved in data acquisition and analysis; N. B. Nordsborg wrote the manuscript and interpreted the data; and J. Martín-Albo and A. Rueda-Robles were involved in data acquisition.

REFERENCES

1. Glancy, B., Hartnell, L. M., Malide, D., Yu, Z. X., Combs, C. A., Connelly, P. S., Subramaniam, S., and Balaban, R. S. (2015) Mitochondrial reticulum for cellular energy distribution in muscle. *Nature* **523**, 617–620
2. Helle, S. C. J., Feng, Q., Aebersold, M. J., Hirt, L., Grüter, R. R., Vahid, A., Sirianni, A., Mostowy, S., Snedeker, J. G., Šarić, A., Idema, T., Zambelli, T., and Kornmann, B. (2017) Mechanical force induces mitochondrial fission. *eLife* **6**, e30292
3. Pernas, L., and Scorrano, L. (2016) Mito-morphosis: mitochondrial fusion, fission, and cristae remodeling as key mediators of cellular function. *Annu. Rev. Physiol.* **78**, 505–531
4. Drake, J. C., Wilson, R. J., and Yan, Z. (2016) Molecular mechanisms for mitochondrial adaptation to exercise training in skeletal muscle. *FASEB J.* **30**, 13–22
5. Franco, A., Kitsis, R. N., Fleischer, J. A., Gavathiotis, E., Kornfeld, O. S., Gong, G., Biris, N., Benz, A., Qvit, N., Donnelly, S. K., Chen, Y., Mennerick, S., Hodgson, L., Mochly-Rosen, D., and Dorn, G. W. I. I. (2016) Correcting mitochondrial fusion by manipulating mitofusin conformations. *Nature* **540**, 74–79
6. Sebastián, D., and Zorzano, A. (2018) Mitochondrial dynamics and metabolic homeostasis. Curr. Opin. Physiol. **3**, 34–40
7. Holloszy, J. O. (1967) Biochemical adaptations in muscle. Effects of exercise on mitochondrial oxygen uptake and respiratory enzyme activity in skeletal muscle. *J. Biol. Chem.* **242**, 2278–2282
8. Meinild Lundby, A. K., Jacobs, R. A., Gehrig, S., de Leur, J., Hauser, M., Bonne, T. C., Flück, D., Dandanell, S., Kirk, N., Kaech, A., Ziegler, U., Larsen, S., and Lundby, C. (2018) Exercise training increases skeletal muscle mitochondrial volume density by enlargement of existing mitochondria and not de novo biogenesis. *Acta Physiol. (Oxf.)* **222**, e12905
9. Huertas, J. R., Al Fazazi, S., Hidalgo-Gutierrez, A., López, L. C., and Casuso, R. A. (2017) Antioxidant effect of exercise: exploring the role of the mitochondrial complex I superassembly. *Redox Biol.* **13**, 477–481
10. Greggio, C., Jha, P., Kulkarni, S. S., Lagarrigue, S., Broskey, N. T., Boutant, M., Wang, X., Conde Alonso, S., Ofori, E., Auwerx, J., Cantó, C., and Amati, F. (2017) Enhanced respiratory chain supercomplex formation in response to exercise in human skeletal muscle. *Cell Metab.* **25**, 301–311, 20
11. Skulachev, V. P. (2001) Mitochondrial filaments and clusters as intracellular power-transmitting cables. *Trends Biochem. Sci.* **26**, 23–29
12. Mishra, P., and Chan, D. C. (2016) Metabolic regulation of mitochondrial dynamics. *J. Cell Biol.* **212**, 379–387
13. Gibala, M. J., MacLean, D. A., Graham, T. E., and Saltin, B. (1998) Tricarboxylic acid cycle intermediate pool size and estimated cycle flux in human muscle during exercise. *Am. J. Physiol.* **275**, E235–E242
14. MacInnis, M. J., and Gibala, M. J. (2017) Physiological adaptations to interval training and the role of exercise intensity. *J. Physiol.* **595**, 2915–2930
15. Psilander, N., Wang, L., Westergren, J., Tonkonogi, M., and Sahlin, K. (2010) Mitochondrial gene expression in elite cyclists: effects of high-intensity interval exercise. *Eur. J. Appl. Physiol.* **110**, 597–606; erratum: 607
16. Cartoni, R., Léger, B., Hock, M. B., Praz, M., Crettenand, A., Pich, S., Ziltener, J. L., Luthi, F., Dériaz, O., Zorzano, A., Gobelet, C., Kralli, A., and Russell, A. P. (2005) Mitofusins 1/2 and ERRalpha expression are increased in human skeletal muscle after physical exercise. *J. Physiol.* **567**, 349–358
17. Fiorenza, M., Gunnarsson, T. P., Hostrup, M., Iaia, F. M., Schena, F., Pilegaard, H., and Bangsbo, J. (2018) Metabolic stress-dependent

regulation of the mitochondrial biogenic molecular response to high-intensity exercise in human skeletal muscle. *J. Physiol.* **596**, 2823–2840
18. Granata, C., Oliveira, R. S., Little, J. P., Renner, K., and Bishop, D. J. (2017) Sprint-interval but not continuous exercise increases PGC-1α protein content and p53 phosphorylation in nuclear fractions of human skeletal muscle. *Sci. Rep.* **7**, 44227
19. Casuso, R. A., Plaza-Díaz, J., Ruiz-Ojeda, F. J., Aragón-Vela, J., Robles-Sanchez, C., Nordsborg, N. B., Hebberecht, M., Salmeron, L. M., and Huertas, J. R. (2017) High-intensity high-volume swimming induces more robust signaling through PGC-1α and AMPK activation than sprint interval swimming in m. triceps brachii. *PLoS One* **12**, e0185494
20. Casuso, R. A., Martínez-López, E., Hita-Contreras, F., Ruiz-Cazalilla, I., Cruz-Díaz, D., and Martínez-Amat, A. (2014) Effects of in-water passive recovery on sprint swimming performance and heart rate in adolescent swimmers. *J. Sports Sci. Med.* **13**, 958–963
21. Bustin, S. A., Benes, V., Garson, J. A., Hellemans, J., Huggett, J., Kubista, M., Mueller, R., Nolan, T., Pfaffl, M. W., Shipley, G. L., Vandesompele, J., and Wittwer, C. T. (2009) The MIQE guidelines: minimum information for publication of quantitative real-time PCR experiments. *Clin. Chem.* **55**, 611–622
22. Picard, M., Gentil, B. J., McManus, M. J., White, K., St Louis, K., Gartside, S. E., Wallace, D. C., and Turnbull, D. M. (2013) Acute exercise remodels mitochondrial membrane interactions in mouse skeletal muscle. *J. Appl. Physiol.* **115**, 1562–1571
23. Picard, M., White, K., and Turnbull, D. M. (2013) Mitochondrial morphology, topology, and membrane interactions in skeletal muscle: a quantitative three-dimensional electron microscopy study. *J. Appl. Physiol.* **114**, 161–171
24. Nielsen, J., Holmberg, H. C., Schrøder, H. D., Saltin, B., and Ortenblad, N. (2011) Human skeletal muscle glycogen utilization in exhaustive exercise: role of subcellular localization and fibre type. *J. Physiol.* **589**, 2871–2885
25. West, M. J. (2012) Estimating volume in biological structures. *Cold Spring Harb. Protoc.* **2012**, 1129–1139
26. Koyano, F., Yamano, K., Kosako, H., Tanaka, K., and Matsuda, N. (2019) Parkin recruitment to impaired mitochondria for nonselective ubiquitylation is facilitated by MITOL. *J. Biol. Chem.* **294**, 10300–10314
27. Schwalm, C., Deldicque, L., and Francaux, M. (2017) Lack of activation of mitophagy during endurance exercise in human. *Med. Sci. Sports Exerc.* **49**, 1552–1561
28. Eisner, V., Lenaers, G., and Hajnóczky, G. (2014) Mitochondrial fusion is frequent in skeletal muscle and supports excitation-contraction coupling. *J. Cell Biol.* **205**, 179–195
29. Mathai, A. S., Bonen, A., Benton, C. R., Robinson, D. L., and Graham, T. E. (2008) Rapid exercise-induced changes in PGC-1alpha mRNA and protein in human skeletal muscle. *J. Appl. Physiol.* **105**, 1098–1105
30. Granata, C., Oliveira, R. S., Little, J. P., Renner, K., and Bishop, D. J. (2016) Training intensity modulates changes in PGC-1α and p53 protein content and mitochondrial respiration, but not markers of mitochondrial content in human skeletal muscle. *FASEB J.* **30**, 959–970
31. Zinner, C., Morales-Alamo, D., Ørtenblad, N., Larsen, F. J., Schiffer, T. A., Willis, S. J., Gelabert-Rebato, M., Perez-Valera, M., Boushel, R., Calbet, J. A., and Holmberg, H. C. (2016) The physiological mechanisms of performance enhancement with sprint interval training differ between the upper and lower extremities in humans. *Front. Physiol.* **7**, 426
32. Boushel, R., Gnaiger, E., Calbet, J. A., Gonzalez-Alonso, J., Wright-Paradis, C., Sondergaard, H., Ara, I., Helge, J. W., and Saltin, B. (2011) Muscle mitochondrial capacity exceeds maximal oxygen delivery in humans. *Mitochondrion* **11**, 303–307
33. Ørtenblad, N., Nielsen, J., Boushel, R., Söderlund, K., Saltin, B., and Holmberg, H. C. (2018) The muscle fiber profiles, mitochondrial content, and enzyme activities of the exceptionally well-trained arm and leg muscles of elite cross-country skiers. *Front. Physiol.* **9**, 1031
34. Larsen, F. J., Schiffer, T. A., Ørtenblad, N., Zinner, C., Morales-Alamo, D., Willis, S. J., Calbet, J. A., Holmberg, H. C., and Boushel, R. (2016) High-intensity sprint training inhibits mitochondrial respiration through aconitase inactivation. *FASEB J.* **30**, 417–427
35. Fealy, C. E., Mulya, A., Lai, N., and Kirwan, J. P. (2014) Exercise training decreases activation of the mitochondrial fission protein dynamin-related protein-1 in insulin-resistant human skeletal muscle. *J. Appl. Physiol.* **117**, 239–245
36. Axelrod, C. L., Fealy, C. E., Mulya, A., and Kirwan, J. P. (2019) Exercise training remodels human skeletal muscle mitochondrial fission and fusion machinery towards a pro-elongation phenotype. *Acta Physiol. (Oxf.)* **225**, e13216
37. De Brito, O. M., and Scorrano, L. (2008) Mitofusin 2 tethers endoplasmic reticulum to mitochondria. *Nature* **456**, 605–610; erratum: 513, 266
38. Cogliati, S., Frezza, C., Soriano, M. E., Varanita, T., Quintana-Cabrera, R., Corrado, M., Cipolat, S., Costa, V., Casarin, A., Gomes, L. C., Perales-Clemente, E., Salviati, L., Fernandez-Silva, P., Enriquez, J. A., and Scorrano, L. (2013) Mitochondrial cristae shape determines respiratory chain supercomplexes assembly and respiratory efficiency. *Cell* **155**, 160–171
39. Del Dotto, V., Mishra, P., Vidoni, S., Fogazza, M., Maresca, A., Caporali, L., McCaffery, J. M., Cappelletti, M., Baruffini, E., Lenaers, G., Chan, D., Rugolo, M., Carelli, V., and Zanna, C. (2017) OPA1 isoforms in the hierarchical organization of mitochondrial functions. *Cell Rep.* **19**, 2557–2571
40. Granata, C., Jamnick, N. A., and Bishop, D. J. (2018) Training-induced changes in mitochondrial content and respiratory function in human skeletal muscle. *Sports Med.* **48**, 1809–1828
41. Otera, H., Wang, C., Cleland, M. M., Setoguchi, K., Yokota, S., Youle, R. J., and Mihara, K. (2010) Mff is an essential factor for mitochondrial recruitment of Drp1 during mitochondrial fission in mammalian cells. *J. Cell Biol.* **191**, 1141–1158
42. Toyama, E. Q., Herzig, S., Courchet, J., Lewis, T. L., Jr., Losón, O. C., Hellberg, K., Young, N. P., Chen, H., Polleux, F., Chan, D. C., and Shaw, R. J. (2016) Metabolism. AMP-activated protein kinase mediates mitochondrial fission in response to energy stress. *Science* **351**, 275–281
43. James, D. I., Parone, P. A., Mattenberger, Y., and Martinou, J. C. (2003) hFis1, a novel component of the mammalian mitochondrial fission machinery. *J. Biol. Chem.* **278**, 36373–36379
44. Gomes, L. C., and Scorrano, L. (2008) High levels of Fis1, a pro-fission mitochondrial protein, trigger autophagy. *Biochim. Biophys. Acta* **1777**, 860–866
45. Shen, Q., Yamano, K., Head, B. P., Kawajiri, S., Cheung, J. T., Wang, C., Cho, J. H., Hattori, N., Youle, R. J., and van der Bliek, A. M. (2014) Mutations in Fis1 disrupt orderly disposal of defective mitochondria. *Mol. Biol. Cell* **25**, 145–159
46. Ørtenblad, N., Nielsen, J., Saltin, B., and Holmberg, H. C. (2011) Role of glycogen availability in sarcoplasmic reticulum Ca2+ kinetics in human skeletal muscle. *J. Physiol.* **589**, 711–725
47. Gaitanos, G. C., Williams, C., Boobis, L. H., and Brooks, S. (1993) Human muscle metabolism during intermittent maximal exercise. *J. Appl. Physiol.* **75**, 712–719
48. Hoppeler, H. (1986) Exercise-induced ultrastructural changes in skeletal muscle. *Int. J. Sports Med.* **7**, 187–204
49. Huertas, J. R., Casuso, R. A., Hernansanz-Agustín, P., and Cogliati, S. (2019) Stay fit, stay young: mitochondria in movement: the role of exercise in the new mitochondrial paradigm. *Oxid. Med. Cell. Longev.* **2019**, 7058350
50. Feng, Q., and Kornmann, B. (2018) Mechanical forces on cellular organelles. *J. Cell Sci.* **131**, jcs218479
51. Gollnick, P. D., and King, D. W. (1969) Effect of exercise and training on mitochondria of rat skeletal muscle. *Am. J. Physiol.* **216**, 1502–1509
52. Gale, J. B. (1974) Mitochondrial swelling associated with exercise and method of fixation. *Med. Sci. Sports* **6**, 182–187
53. Terjung, R. L., Baldwin, K. M., Molé, P. A., Klinkerfuss, G. H., and Holloszy, J. O. (1972) Effect of running to exhaustion on skeletal muscle mitochondria: a biochemical study. *Am. J. Physiol.* **223**, 549–554

Received for publication February 6, 2019.
Accepted for publication July 16, 2019.